AFRL-RX-WP-JA-2014-0232

# CHARACTERIZATION OF DEGRADATION USING REFLECTANCE SPECTROSCOPY (POSTPRINT)

**A. K. Criner**
**University of Dayton Research Institute**

**A. J. Cherry**
**Southwestern Ohio Council for Higher Education**

**T. D. Katter**
**Universal Technologies Corporation**

**A. T. Cooney**
**AFRL/RXCA**

**AUGUST 2013**
**Interim Report**

STINFO COPY

**AIR FORCE RESEARCH LABORATORY**
**MATERIALS AND MANUFACTURING DIRECTORATE**
**WRIGHT-PATTERSON AIR FORCE BASE, OH 45433-7750**
**AIR FORCE MATERIEL COMMAND**
**UNITED STATES AIR FORCE**

# NOTICE AND SIGNATURE PAGE

|  |  |
|---|---|
| //Signature// | //Signature// |
| JOHN T. WELTER, Project Engineer | STEPHAN M. RUSS, Chief |
| Materials State Awareness & Supportability Branch | Materials State Awareness & Supportability Branch |
| Structural Materials Division | Structural Materials Division |

_____//Signature//_____
ROBERT T. MARSHALL, Deputy Chief
Structural Materials Division
Materials and Manufacturing Directorate

# REPORT DOCUMENTATION PAGE

Public reporting burden for this collection of information is estimated to average 1 hour per response, including the time for reviewing instructions, searching existing data sources, gathering and maintaining the data needed, and completing and reviewing this collection of information. Send comments regarding this burden estimate or any other aspect of this collection of information, including suggestions for reducing this burden to Defense, Washington Headquarters Services, Directorate for Information Operations and Reports, 1215 Jefferson Davis Highway, Suite 1204, Arlington, VA 22202-4302. Respondents should be aware that notwithstanding any other provision of law, no person shall be subject to any penalty for failing to comply with a collection of information if it dows not display a currently valid OMB control number. **PLEASE DO NOT RETURN YOUR FORM TO THE ABOVE ADDRESS.**

| 1. REPORT DATE (DD-MM-YYYY) August 2013 | 2. REPORT TYPE Interim | 3. DATES COVERED *(From – To)* 25 June 2009 – 21 July 2013 |
|---|---|---|
| **4. TITLE AND SUBTITLE** CHARACTERIZATION OF DEGRADATION USING REFLECTANCE SPECTROSCOPY (POSTPRINT) | | **5a. CONTRACT NUMBER** FA8650-09-D-5224-0001 |
| | | **5b. GRANT NUMBER** |
| | | **5c. PROGRAM ELEMENT NUMBER** 62102F |
| **6. AUTHOR(S)** (see back) | | **5d. PROJECT NUMBER** 4347 |
| | | **5e. TASK NUMBER** |
| | | **5f. WORK UNIT NUMBER** X0SU |
| **7. PERFORMING ORGANIZATION NAME(S) AND ADDRESS(ES)** (see back) | | **8. PERFORMING ORGANIZATION REPORT NUMBER** |
| **9. SPONSORING / MONITORING AGENCY NAME(S) AND ADDRESS(ES)** Air Force Research Laboratory Materials and Manufacturing Directorate Wright Patterson Air Force Base, OH 45433-7750 Air Force Materiel Command United States Air Force | | **10. SPONSOR/MONITOR'S ACRONYM(S)** AFRL/RXCA |
| | | **11. SPONSOR/MONITOR'S REPORT NUMBER(S)** AFRL-RX-WP-JA-2014-0232 |

**12. DISTRIBUTION / AVAILABILITY STATEMENT**
Distribution A. Approved for public release; distribution unlimited. This report contains color.

**13. SUPPLEMENTARY NOTES**

**14. ABSTRACT**
A semi-classical model of the reflectance of a complex material is modeled. Model selection techniques using this reflectance model are developed to detect molecular vibration modes measured using infrared spectroscopy. An inverse problem methodology is then used to ascertain the underlying vibrational modes associated with varying concentrations of different chemical species. These two techniques are developed to characterize the extent of material degradation through the detection of spectra associated with the chemical processes underlying the degradation process. These methods are validated using data from samples of ceramic matrix composites. The samples considered were exposed to varying amounts of thermal treatment to ascertain the effectiveness of these methods to detect degradation.

**15. SUBJECT TERMS**
resolution, eddy current, mechanical, permanent magnet

| 16. SECURITY CLASSIFICATION OF: | | | 17. LIMITATION OF ABSTRACT | 18. NUMBER OF PAGES | 19a. NAME OF RESPONSIBLE PERSON *(Monitor)* John T. Welter |
|---|---|---|---|---|---|
| **a. REPORT** Unclassified | **b. ABSTRACT** Unclassified | **c. THIS PAGE** Unclassified | SAR | 13 | **19b. TELEPHONE NUBER** *(include area code)* (937) 255-9798 |

# REPORT DOCUMENTATION PAGE Cont'd

**6. AUTHOR(S)**

A. K. Criner
University of Dayton Research Institute

A. J. Cherry
Southwestern Ohio Council for Higher Education

T. D. Katter
Universal Technologies Corporation

A. T. Cooney
AFRL/RXCA

**7. PERFORMING ORGANIZATION NAME(S) AND ADDRESS(ES)**

University of Dayton Research Institute
Structural Integrity Division
300 College Park Drive
Dayton OH 45469

Southwestern Ohio Council for Higher Education
Dayton, OH 45420

Universal Technologies Corporation
Dayton, OH 45432

AFRL/RXCA
Air Force Research Laboratory
Materials and Manufacturing Directorate
Wright-Patterson Air Force Base, OH 45433-7750

# Characterization of Degradation Using Reflectance Spectroscopy

A. K. Criner*, A.J. Cherry†, A.T. Cooney,** and T.D. Katter‡

*University of Dayton Research Institute, Dayton, OH 45469, USA
†Southwestern Ohio Council for Higher Education, Dayton, OH 45420, USA
**Materials State Awareness & Supportability Branch, Air Force Research Laboratory, WPAFB 45433, USA
‡Universal Technologies Corporation, Dayton, OH 45432, USA

**Abstract.** A semi-classical model of the reflectance of a complex material is modeled. Model selection techniques using this reflectance model are developed to detect molecular vibration modes measured using infrared spectroscopy. An inverse problem methodology is then used to ascertain the underlying vibrational modes associated with varying concentrations of different chemical species. These two techniques are developed to characterize the extent of material degradation through the detection of spectra associated with the chemical processes underlying the degradation process. These methods are validated using data from samples of ceramic matrix composites. The samples considered were exposed to varying amounts of thermal treatment to ascertain the effectiveness of these methods to detect degradation.

**Keywords:** Reflectance Spectroscopy, Optical Constants, Fourier Infrared Spectroscopy, Data Analysis

## INTRODUCTION

Evaluation of ceramic matrix composites is the main motivation for this study, however, we hope that these methods or methods like these could eventually be applied to other materials. Degradation due to oxidation takes place in ceramic matrix composite before an actual damage occurs. This degradation causes these materials to become brittle which leads to catastrophic failure.

Ceramic matrix composite have a multiscale geometry which causes exact modeling of the components to be nonviable. The mesoscale structure includes tows which are woven into cross plies through the matrix; this is on the 1 mm scale. The tows are composed of fiber bundles which are on the scale of 100 $\mu$m. An approximate description is depicted in Figure 1. The degradation that we are concerned with occurs at the scale of the individual fibers ($\sim$10 nm), see Figure 2. For nondestructive evaluation applications, the exact geometry is not available *a priori*, would be too computationally intensive to include in models, and is not of primary interest. Models of very different forms can be deduced from various and assorted assumptions though none of these can expected to be exact [1]. In our analysis, we used model selection results to make data driven choices between two models that we used to analyze the data.

A further complication in this problem is related to nature of the degradation that we seek to characterize. At high temperatures, air causes the formation of oxides in ceramic matrix composites. This oxidation at small levels (before it is observable by most other methods) causes the material to be brittle [2]. The degradation can be observed by transmission electron microscopy and electron energy loss spectroscopy [3]. These methods are not capable of in field inspection so we seek a method that could be performed in field. Fourier transform infrared (FTIR) devices have been developed with in field inspection capabilities [4].

Spectroscopy is a very common technique in many fields. It is a ubiquitous tool in control processes in the food production, medicine and petroleum production, to name a few [4]. It is also used in detection in chemistry and astronomy [5]. Many of the fields consider applications where Beer's law applies which allows the data to be transformed to a linear model. In these cases, all the techniques for linear models may be applied such as PCA and PLS [6, 7]. These techniques can be used for data from nonlinear models however the results will not correspond to a physically meaningful quantity which is our goal. To obtain inference about small chemical changes, we use an inverse problem model based approach on the data that we collected.

1
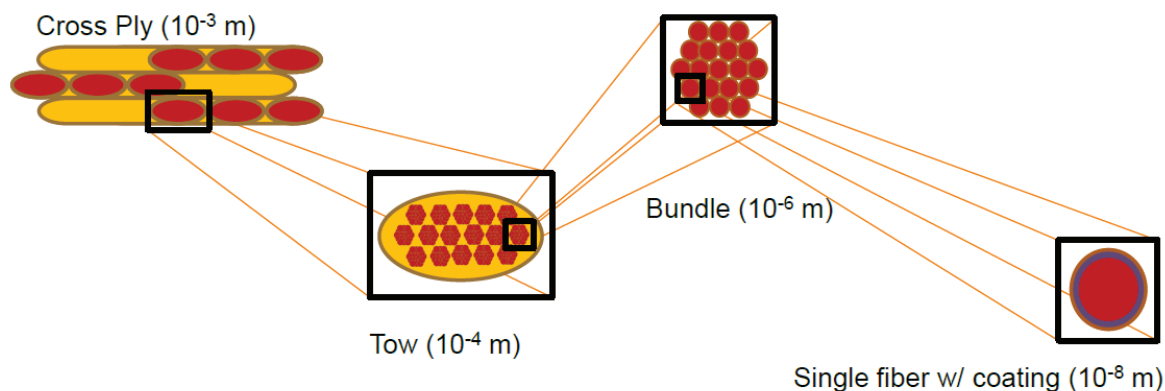
**FIGURE 1.** An example diagram of the multiscale geometry of ceramic matrix composites.
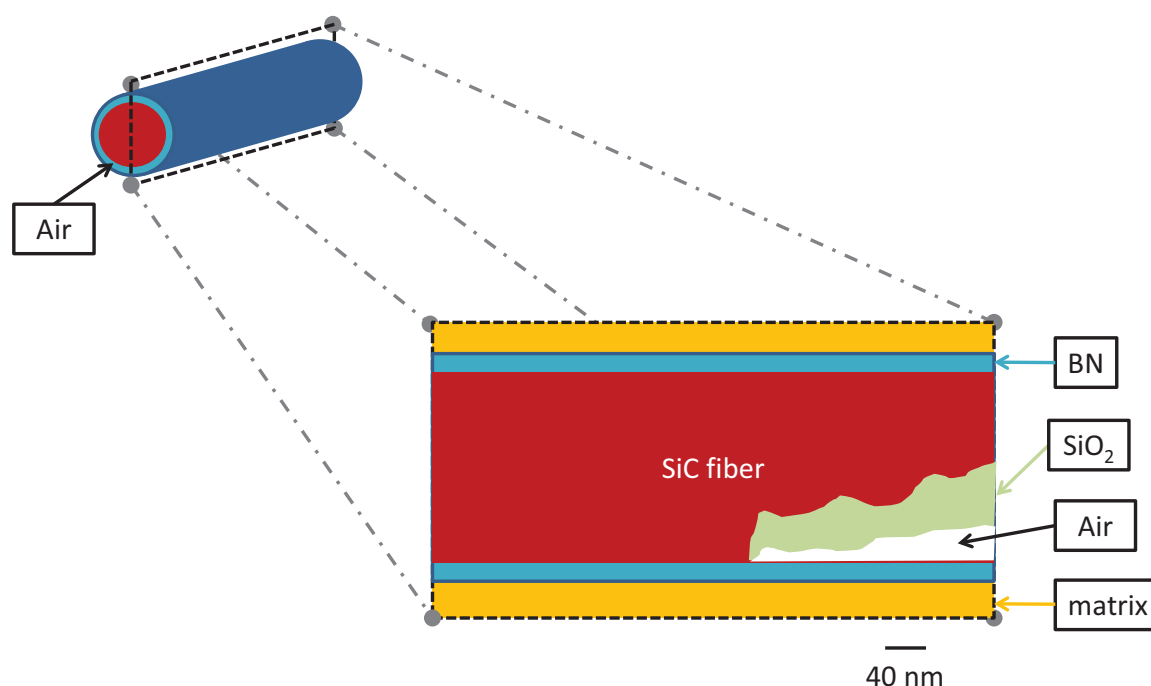


**FIGURE 2.** Diagram of the degradation.

## EXPERIMENTAL DESCRIPTION

IR spectroscopy was performed on silicon nitride carbon based CMC samples before and after heat treatment. MIR measurements were made using a Bruker Vertex 80v FTIR attached to a Harrick Omni-Spec probe. The probe made surface contact where 45-degree reflection measurements were collected and compared to a mirror reference. The samples were 15.7 x 1.3 x 0.2 cm in dimension. Each sample was divided along its length into 11 blocks of equal area. Prior to measuring a sample, reference intensity data was obtained, and then an intensity measurement was collected in the approximate center of each of the 11 blocks. This procedure was considered one trial, and was repeated for the second and third trials. The reflectance data was calculated as the ratio of the intensity measurement from the sample to the intensity measurement of the reference.

2
Distribution A. Approved for public release; distribution unlimited.

**TABLE 1.** Acquisition parameters.

| | | # of pts | 1st Pt (1/cm) | 2nd Pt (1/cm) | Resolution | Sample scans |
|---|---|---|---|---|---|---|
| Baseline | Sample 13 | 5807 | 5998.352276 | 399.247241 | 8 | 16 |
| | Sample 16 | 5807 | 5998.352276 | 399.247241 | 8 | 16 |
| Heat 10H | Sample 4 | 14787 | 7499.386893 | 369.834099 | 4 | 16 |
| | Sample 16 | 14787 | 7499.386893 | 369.834099 | 4 | 16 |
| | Sample 32 | 14787 | 7499.386893 | 369.834099 | 4 | 16 |
| Heat 100H | Sample 1 | 14787 | 7499.386893 | 369.834099 | 4 | 16 |
| | Sample 13 | 5807 | 5998.352276 | 399.247241 | 8 | 16 |
| | Sample 29 | 14787 | 7499.386893 | 369.834099 | 4 | 16 |

Baseline data was collected on samples 13 and 16 using the following specifications: 5807 points over a frequency range of 5998.35 to 399.25 cm-1 with a resolution of 8 cm-1.

Three samples of SiNC (samples 4, 16, and 32) underwent heat treatments of 1200 deg. C for 10 hours. MIR data was collected on these samples using the same method as before except under the following specifications: 14787 points over a frequency range of 7499.39 to 369.83 cm-1 with a resolution of 4 cm-1.

In addition, three samples of SiNC (samples 1 and 29) were exposed to heat treatments of 1200 deg. C for 100 hours. These samples were inspected in the same manner as samples 4, 16, and 32. Sample 13 was exposed to the same heat treatment as samples 1 and 29 but was inspected using the same specifications used to collect the baseline data. A summary of the collected data is given in Table 1.

## DATA ANALYSIS

To relate changes in data to such small physical changes, we need to analyze the data with models that give reflectance from parameters that relate to chemical changes. We would like these to result in information about the underlying amounts of chemicals and their phase. An example of the changes in the data is given in Figure 3

We first use standard optical results to model the reflectance and the refractive index of the material. Throughout this description, we use the notation in Table 2. The two polarizations of the reflectivity are given by

$$r_\perp(x;q^{(N)}) = \frac{n_A \cos\theta_I - \left(\tilde{n}^2(x;q^{(N)}) - n_A^2 \sin^2\theta_I\right)^{\frac{1}{2}}}{n_A \cos\theta_I + \left(\tilde{n}^2(x;q^{(N)}) - n_A^2 \sin^2\theta_I\right)^{\frac{1}{2}}}$$

(1)

$$r_\parallel(x;q^{(N)}) = \frac{n_A \left(1 - \frac{n_A^2}{\tilde{n}^2(x;q^{(N)})} \sin^2\theta_I\right)^{\frac{1}{2}} - \tilde{n}(x;q^{(N)}) \cos\theta_I}{n_A \left(1 - \frac{n_A^2}{\tilde{n}^2(x;q^{(N)})} \sin^2\theta_I\right)^{\frac{1}{2}} + \tilde{n}(x;q^{(N)}) \cos\theta_I},$$

(2)

which is derived using Snell's law and Fresnel's law [8]. The total reflectance is given by the the average of the two polarizations of the reflectance. These are the moduli squared of the complex two polarizations of the complex reflectivity:

$$R(x;q^{(N)}) = \frac{1}{2}\left(\left|r_\perp(x;q^{(N)})\right|^2 + \left|r_\parallel(x;q^{(N)})\right|^2\right),$$

(3)

where $|\cdot|$ is the modulus of the complex number ($z = x + iy$ then $|z| = \sqrt{x^2 + y^2}$) [8].

The refractive index of a material depends on its complex dielectric constant through the following relation:

$$\tilde{n}^2(x) = \tilde{\varepsilon}^2(x).$$

3

Distribution A. Approved for public release; distribution unlimited.
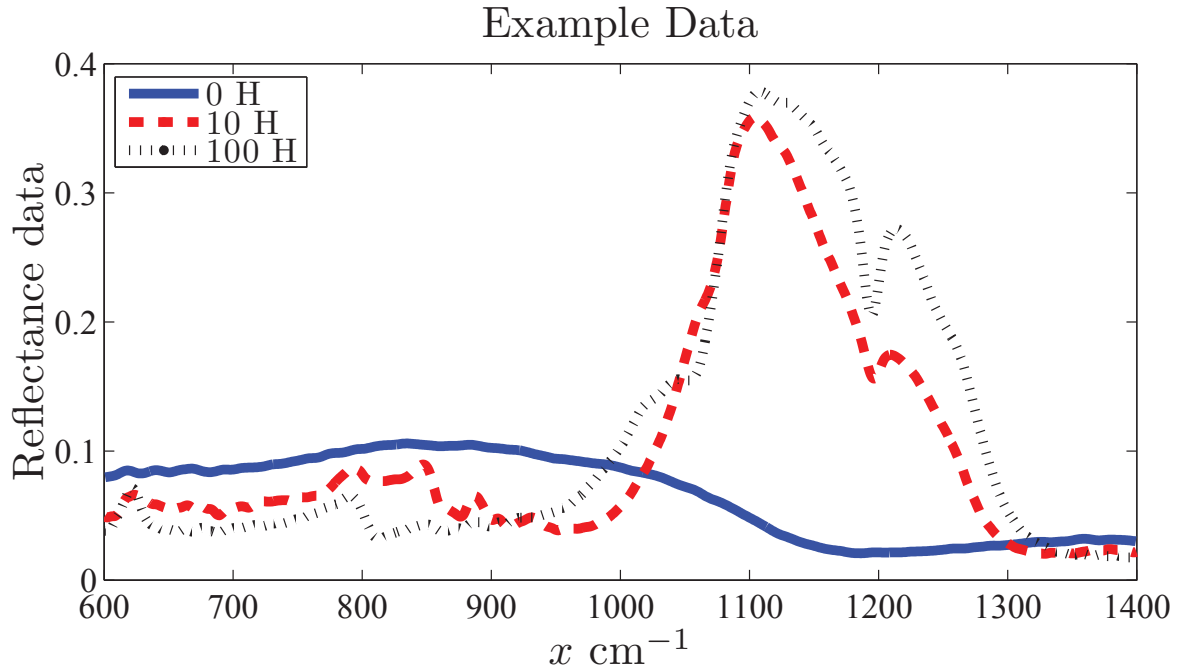
## Example Data



**FIGURE 3.** Example data from randomly selected data sets.

**TABLE 2.** Notation.

| Symbol | Parameter | Value |
|--------|-----------|-------|
| $\theta_I$ | Incident angle of beam | 45 degrees |
| $n_A$ | Refractive index of surroundings | 1 |
| $x$ | Wave number | Dependent variable, varies from $400 - 1400 \text{ cm}^{-1}$ |
| $\tilde{\varepsilon}$ | Dielectric constant or permittivity (complex number) | Varies with wave number |
| $\tilde{n}$ | Refractive index of material (complex number) | Depends on $\tilde{\varepsilon}$ |
| $R_\perp$ | Perpendicular polarization reflectance | Depends on $\tilde{n}$, Snell/Fresnel |
| $R_\parallel$ | Parallel polarization reflectance | Depends on $\tilde{n}$, Snell/Fresnel |
| $R$ | Total Reflectance | Average of $R_\perp$ and $R_\parallel$ |

We model the dielectric constant as a function which is based on assumptions about molecular motions. There have been many models proposed for the dielectric constant which vary regarding form, and number of variables. We will focus on models that use springs (or *oscillators*) to model molecular vibrations. We will denote $\tilde{\varepsilon}(x)$ the complex dielectric function with real and imaginary parts $\varepsilon_1$ and $\varepsilon_2$, respectively,

$$\tilde{\varepsilon}(x) = \varepsilon_1(x) + i\varepsilon_2(x). \tag{4}$$

The dielectric constant has dependent variable wave number $x \text{ cm}^{-1}$. The classical oscillator model is given by

$$\tilde{\varepsilon}(x) = \varepsilon_\infty + \sum_{j=1}^{N} \frac{A_j}{(\omega_j^2 - x^2) - i\Gamma_j x}, \tag{5}$$

where $N$ is the number of oscillators, $\omega_j$ is the resonant frequency, $\Gamma_j$ is the broadening, and $A_j$ is the product of the strength and the number of molecules of that oscillator type. This is known as the Lorentz model in dispersion analysis

4

Distribution A. Approved for public release; distribution unlimited.

and is most appropriate for crystalline systems where the environment is the same for oscillators of the same kind [9]. Efimov proposed a model where the resonant frequency is normally distributed and broadening is the same for all the oscillators [1]. When the standard deviation is much larger than the broadening, this model can be approximated by

$$\varepsilon_2(x) = \sum_{j=1}^{N} \frac{A_j}{\sqrt{2\pi\Delta\omega_j}} e^{-\frac{1}{2}\left(\frac{x-\omega_{0j}}{\Delta\omega_j}\right)^2}$$

(6)

$$\varepsilon_1(x) = \varepsilon_\infty + H.T.\varepsilon_2(x),$$

where H.T. refers to the Hilbert transform [10, 9].

We analyzed our data sets with these two models. For $N \in \{1, 2, 3, \ldots 20\}$, we estimated the parameters in the above models by minimizing the residual sum of squares. We used Aikake information criterion to choose between Lorentz and Gaussian models. For almost all data sets and oscillator numbers, the curve fit was better for the Gauss model than the Lorentz model. We present the results for Gaussian model in the remainder of this manuscript [11].
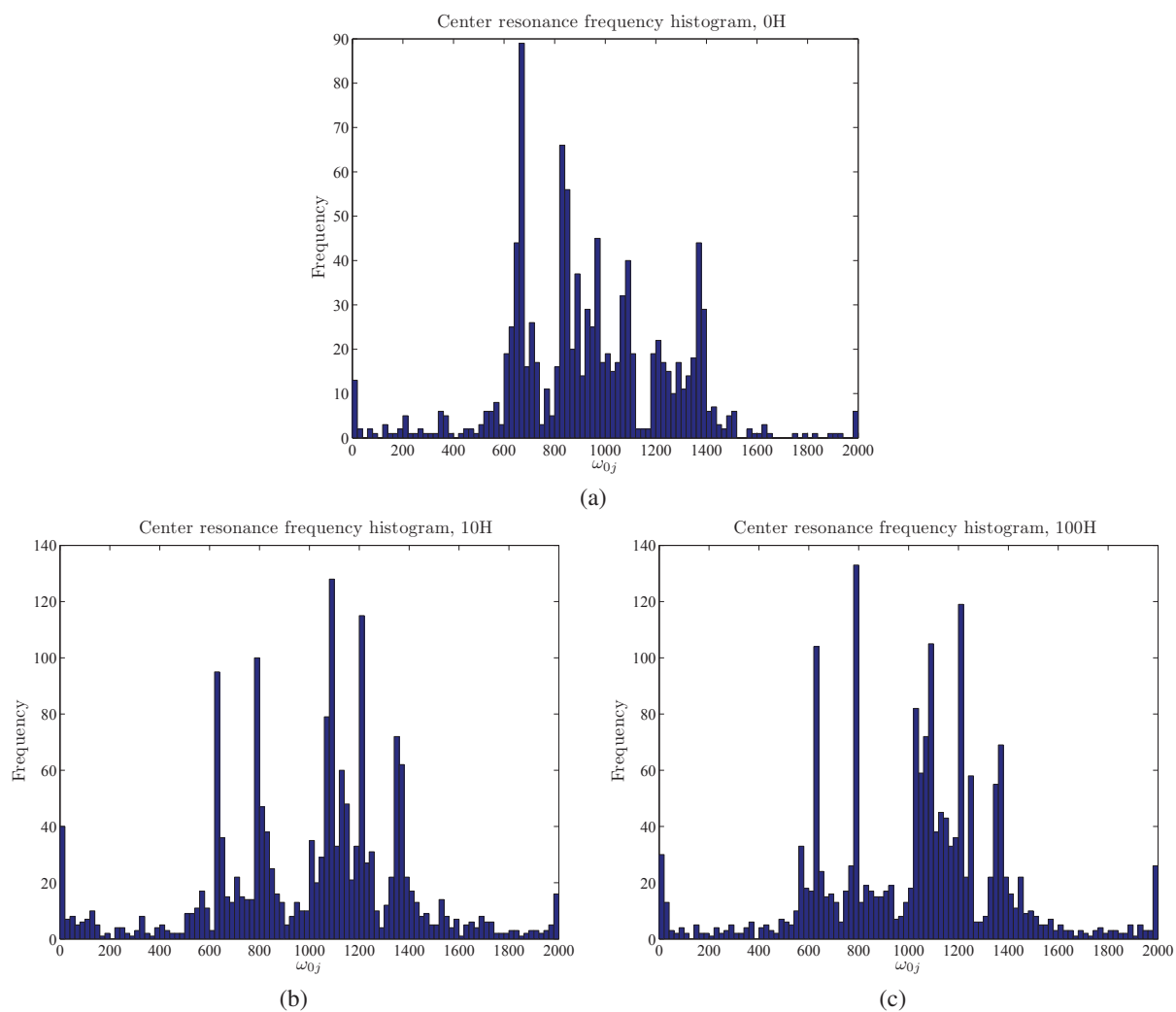
## RESULTS

The models that we chose do not appear to fit the data especially well. Indications of this were observed in poor fits of the curves, many local minima which caused the minimization of the residual sum of squares to be difficult (we used implicit filtering [12]), and the large variation in parameter fits across (a) samples, (b) locations and (c) trials. We have presented histograms of the estimated parameters in Figures 4-6 (a)-(c). There is a large variation of the estimated parameters for all of the estimated parameters. Often in spectroscopy, the estimated resonant frequencies ($\omega_{0j}$'s) are used to identify chemical species and the amplitudes ($A_j$'s) are used to determine the amount. In Figures 4 (a)-(c), we see that there are regions of concentration of resonant frequencies but exactly how many there are is not discernible. There does appear to be a change in resonant frequency between the baseline samples (in Figure 4(a)), and the treated samples. The randomness of these make the exact differences difficult to discern and impossible to relate to exact chemical phases. There is a large variation in the estimates of the parameters $A_j$ and $\Delta\omega_j$ though there are less regions of high concentrations as in the estimates of $\omega_{0j}$.
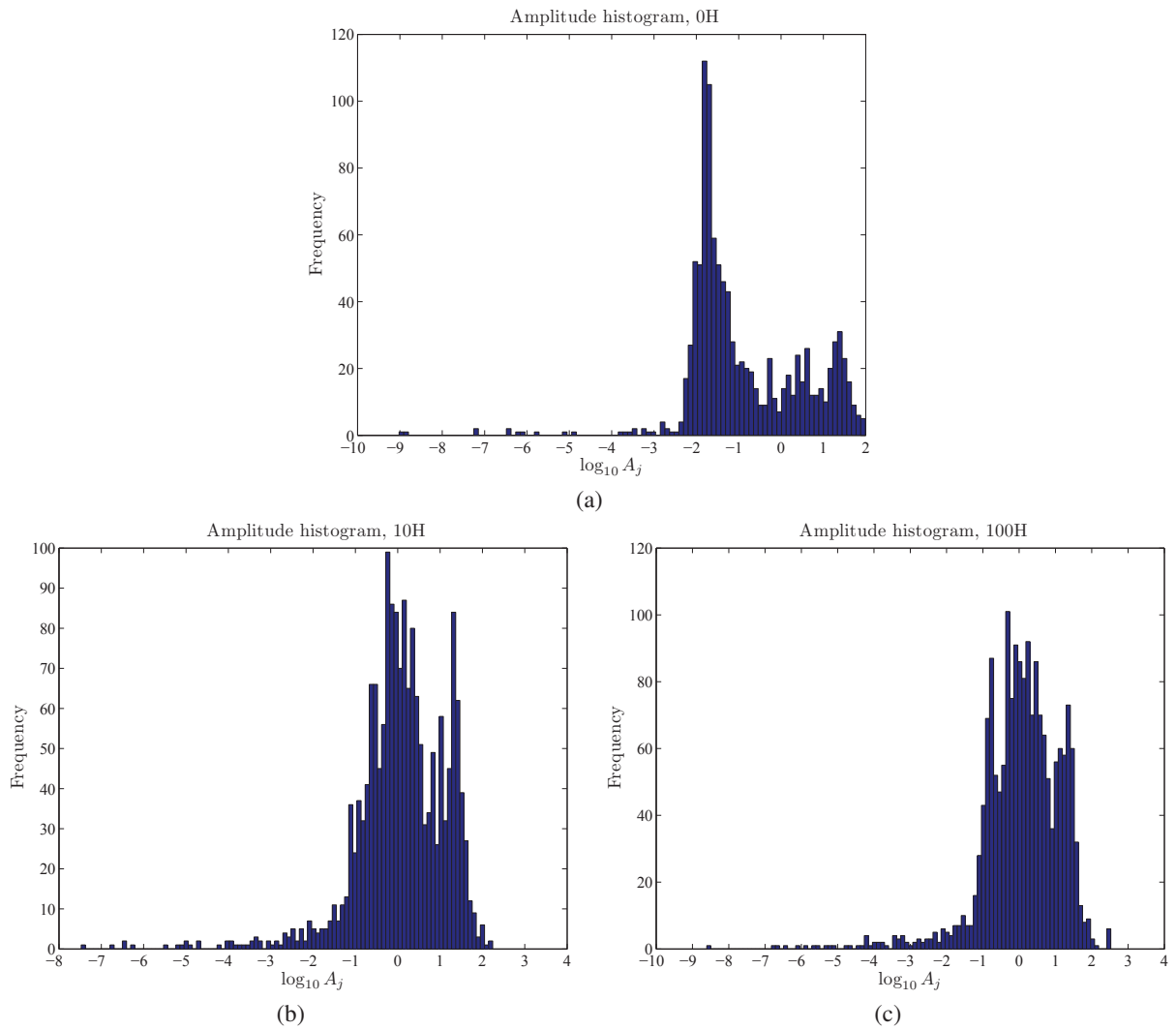
## FUTURE WORK

The results of the our data analysis did indicate differences between the different treatment levels. The apparent randomness of the estimates themselves hindered interpretation of these changes. There could be several causes of this issue. We could be fitting model discrepancy with extra oscillators. We will first try to relax the assumption that $\Gamma_j >> \Delta\omega_j$ that we made in going from the Efimov model to the Gaussian model (6) (as in [9]). This model has been validated for different kinds of glass which leads us to believe it will fit our data better and give us easier to interpret results.
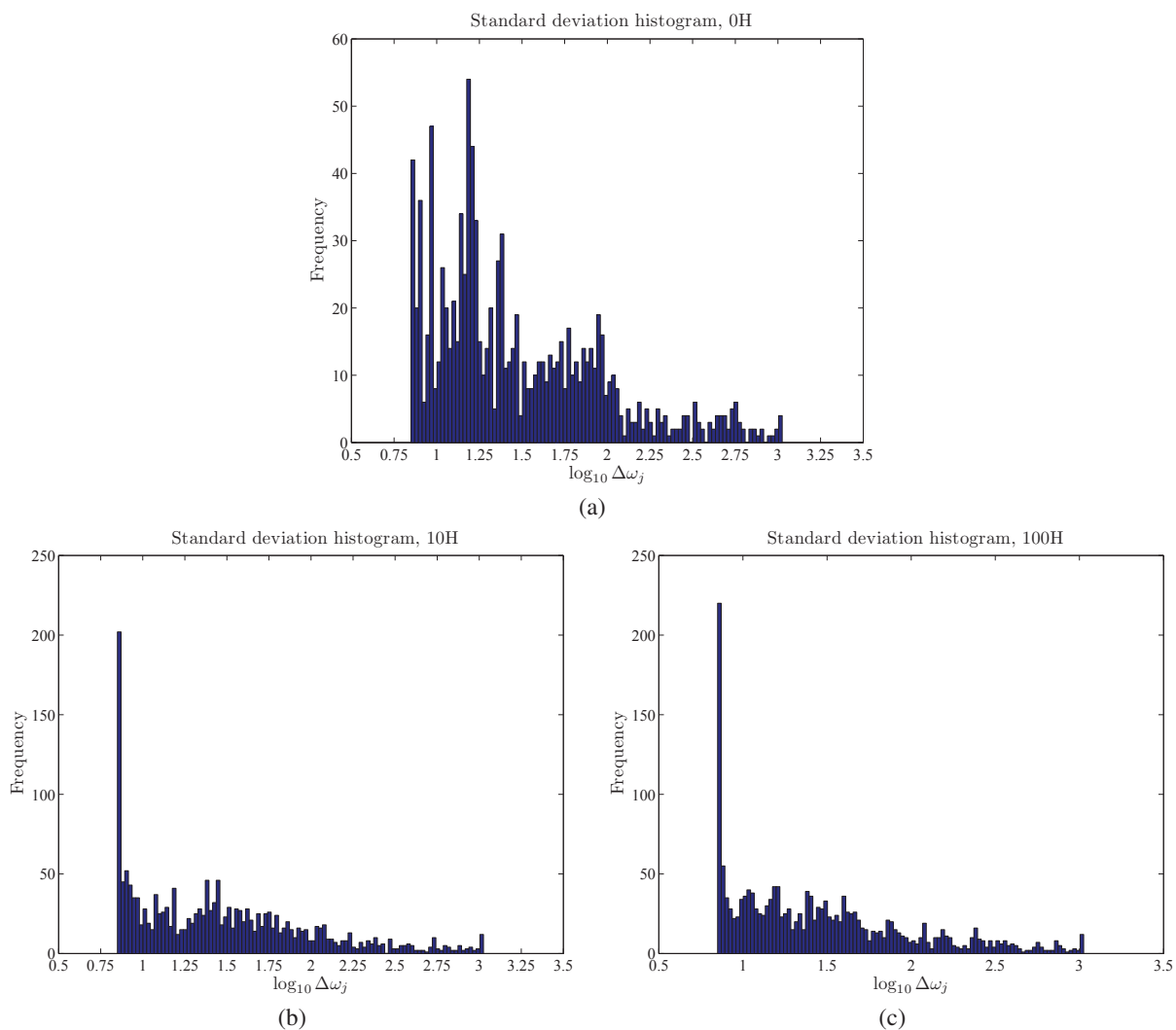
## ACKNOWLEDGMENTS

5

Distribution A. Approved for public release; distribution unlimited.

**FIGURE 4.** Histogram of $\omega_{0j}$ for 100 hour treated data set.

Distribution A. Approved for public release; distribution unlimited.

**FIGURE 5.** Histogram of $\log_{10} A_j$ for 100 hour treated data set.

7
Distribution A. Approved for public release; distribution unlimited.

Standard deviation histogram, 0H

(a)

Standard deviation histogram, 10H

(b)

Standard deviation histogram, 100H

(c)

**FIGURE 6.** Histogram of $\Delta\omega_j$ for 100 hour treated data set.

8
Distribution A.  Approved for public release; distribution unlimited.

# REFERENCES

1.  A. Efimov, *Optical Constants of Inorganic Glasses*, Laser and Optical Science and Technology Series, CRC Press, 1995.
2.  F. E. Heredia, J. C. McNulty, F. W. Zok, and A. G. Evans, *Journal of the American Ceramic Society* **78**, 2097–2100 (1995).
3.  B. W. Sheldon, E. Y. Sun, S. R. Nutt, and J. J. Brennan, *Journal of the American Ceramic Society* **79**, 539–543 (1996).
4.  R. Mukhopadhyay, *Analytical Chemistry* **76**, 369–A (2004).
5.  P. Griffiths, and J. A. De Haseth, *Fourier transform infrared spectrometry*, vol. 171, John Wiley & Sons, 2007.
6.  L. Norgaard, A. Saudland, J. Wagner, J. Nielsen, L. Munck, and S. Engelsen, *Applied Spectroscopy* **54**, 413–419 (2000).
7.  *Analytica Chimica Acta* **635**, 45 – 52 (2009).
8.  D. Griffiths, *Introduction to Electrodynamics*, Prentice-Hall, Inc, 1999, 3rd edn.
9.  S. A. MacDonald, C. R. Schardt, D. J. Masiello, and J. H. Simmons, *Journal of non-crystalline solids* **275**, 72–82 (2000).
10. C. Keefe, *Journal of molecular spectroscopy* **205**, 261–268 (2001).
11. H. Akaike, *Automatic Control, IEEE Transactions on* **19**, 716 – 723 (1974).
12. C. Kelley, *Implicit Filtering*, Software, Environments and Tools, Society for Industrial and Applied Mathematics, 2011.

9

Distribution A. Approved for public release; distribution unlimited.